Physicochem. Probl. Miner. Process., 58(6), 2022, 152164

http://www.journalssystem.com/ppmp

Physicochemical Problems of Mineral Processing

ISSN 1643-1049

Comparison of the depression effect of two thiol depressants on the separation of specularite and aegirite

Mingyang Li [1,2,3], Chen Zhang [3], Xiangpeng Gao [3], Xian Xie [1], Xiong Tong [1]

[1] Faculty of Land Resource Engineering, Kunming University of Science and Technology, Kunming 650093, China

[2] State Key Laboratory of Complex Nonferrous Metal Resources Clean Utilization, Kunming 650093, China

[3] School of Metallurgical Engineering, Anhui University of Technology, Ma'anshan 243002, China

Corresponding authors: kgxianxie@126.com (X. Xie); kgxiongtong@163.com (X. Tong)

Abstract: In this work, two thiol-type reagents, thioglycolic acid (TGA) and mercaptopropionic acid (MPA), were firstly exploited and compared as aegirite depressants with sodium oleate (NaOl) as the collector to separate specularite from aegirite by flotation. The adsorption performances and mechanisms of TGA and MPA on aegirite surface were investigated via flotation experiments, Zeta potential tests, adsorption measurements, contact angle dimensions, and surface characterizations. The results of flotation indicated that TGA and MPA exhibited a considerable depression impact on the flotation of aegirite but little effect on specularite. TGA depicted more excellent depression performance than MPA, which was confirmed by HLB calculation. The results demonstrated that TGA and MPA favorably adsorbed on aegirite surface instead of specularite, hindering the subsequent adsorption of NaOl on specularite and resulting in the surface being hydrophilic. XPS results revealed that TGA and MPA were significantly adsorbed on the surface of aegirite through an interaction between the carboxyl and thiol groups of the depressants and the Si and Fe on the surface of aegirite.

Keywords: aegirite, specularite, flotation, depressant, iron-bearing silicate

1. Introduction

Iron ore is the primary raw material for steel, with iron ore resources being continuously mined and utilized, the research of separation of low-grade refractory iron ores have become an important channel for the utilization of iron ore resources (Filippov, 2013; Fu, 2018; Li, 2020). Among the refractory iron ores, one of the hardest ores to separate is iron-bearing silicates type iron ore, which includes a huge number of gangue minerals such as aegirite, chlorite, and amphibole (Wen, 2013; Pereira, 2021). Aegirite ($FeNaSi_2O_6$) belongs to the subgroup of clinopyroxene, which is a typical single-chain iron-bearing silicate mineral, often associated with iron oxide ore (Li, 2019; Li, 2020). Due to the existing of element iron in the crystal lattice of aegirite, the surface properties and floating characteristics between aegirite and iron oxide ore (e.g. specularite and hematite) is extraordinarily similar, which brings great difficulty to the separation of such ores.

Flotation is considered to be one of the most effective and widely used methods of iron ore beneficiation (Zhang, 2019; Yang, 2022; Rocha, 2019). Although reverse flotation has many advantages, for example: the process is simple, the changes of factors such as ore composition, the slime content and have little influence on flotation, and the concentrate is easy to concentrate and filter (Yao, 2016; Shrimali, 2016; Poperechnikova, 2017; Luo, 2016). The conventional reverse flotation depressant starch show strong depression effect both on aegirite and specularite, due to that aegirite can form strong chemical complexes with starch molecules (Veloso, 2018; Li, 2019; Li, 2020; Huang, 2012). In comparison, direct anionic flotation is a very attractive way to enrich iron ore associated with iron-bearing silicate mineral, but the enrichment efficient is poor due to the low selectivity of flotation reagents.

The inhibiting ability and selectivity of a depressant is critical for achieving an optimum outcome in iron ore flotation. In recent years, the performance and mechanism of action of various types of depressants have been extensively researched (Montes-Sotomayor, 1998; Moreira, 2017; Li, 2019). Thiol-

DOI: 10.37190/ppmp/152164

containing depressants were mainly developed as sulfide ore depressants, such as thioglycolic acid (Gibbs, 1948; Liu, 1985), 2,3-disulfanylbutanedioic acid (Li, 2015), disodium carboxymethyltrithiocarbonate (Yin, 2017), l-cysteine (Yin, 2019) and dithiothreitol (Yan, 2021), and these reagents were proved effective in flotation separation.

Due to that silicon-oxide-tetrahedron's electron attracting ability of aegirite is obvious stronger than that of O ions in specularite. This results in that the electron cloud density of Fe ions in aegirite is lower than that of surface. Therefore, in the adsorption process, thiol-containing depressants should be capable of supplying electrons suffers a smaller repulsive force from the t2g orbit of Fe in aegirite than that of specularite. Compared to specularite, thiol-containing depressants are more likely to adsorb on aegirite surface.

Thioglycolic acid (TGA) and mercaptopropionic acid (MPA), as shown in Fig.1, are the representative thiol depressants. However, a systematic research on specularite/aegirite separation using TGA or MPA as the selective depressant and the depression performance difference between these two regents has not been studied yet. In this work, TGA and MPA were explored as efficient aegirite depressants for selective flotation of specularite (Fe_2O_3) from aegirite. Characterization methods, including Zeta potential, contact angle and XPS detection, were applied to compare and unveil their depression mechanism.

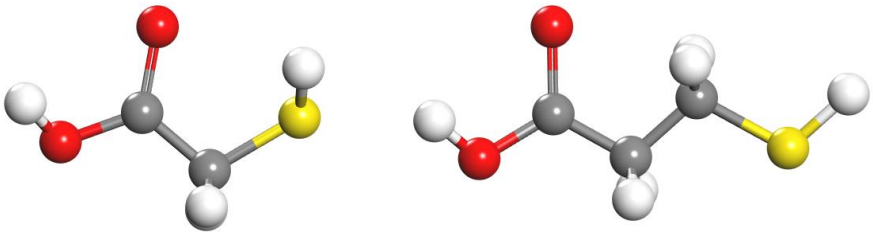

TGA MPA

Fig. 1. The molecular configurations of depressant TGA and MPA (the colour representation is as follows: white-hydrogen atoms; grey-carbon atoms; red-oxygen atoms; yellow-sulfur atoms)

2. Materials and methods

2.1. Materials

The single mineral samples (aegirite and specularite) were obtained from Inner Mongolia and Anhui, China, respectively. For the preparation of single mineral samples, firstly, the selected high-grade ore lumps were broken and handpicked to eliminate visible impurities. Then the impurity-removed samples proceed to being ground and being dried in an agate mortar. Finally, the samples were sieved to different size fractions, among which the size fraction between 37 μm and 74 μm were used for flotation, while the size fraction less than 37 μm were further ground to less than 2 μm for other experiments. For the flotation samples, the d_{80} of aegirite and specularite was 52 μm and 65 μm, respectively. The analytical-grade collector sodium oleate (NaOl), depressant thioglycolic acid (TGA) and mercaptopropionic acid (MPA), pH modifiers HCl and NaOH were all supplied by Adamas-beta® (Shanghai Titan Scientific Co. Ltd.). For all tests, deionized water with a resistivity of 18.2 MΩ·cm was employed.

2.2. Methods

2.2.1. Characterization of materials

The phase and chemical composition of the two minerals were detected using ARL Advant'X Intellipow XRF analyzer (Thermo Fisher Scientific, USA) and D8 Advance X-ray powder diffractometer (Bruker Instruments Ltd., Germany), respectively. The chemical composition results were shown in table 1. The specularite sample show high purity with iron oxides at 95.74% by weight. The sample aegirite was mainly composed of metallosilicates, of which Si, Fe, Na, Ca, Al and Mg silicates accounted for 91.7%

of the total mineral. Fig. 2 depicts the XRD patterns of the two minerals. Combining the results of chemical composition and XRD analysis, the purity of the mineral samples meets the analytical requirements of various subsequent experiments.

Table 1. Chemical composition of aegirite and specularite

Sample	Chemical composition content (%)						
	Fe_2O_3	SiO_2	Al_2O_3	MgO	TiO_2	CaO	Na_2O
Specularite	95.74	3.36	0.38	0.23	0.08	0.04	-
Aegirite	27.90	48.21	0.69	0.24	-	2.42	12.24

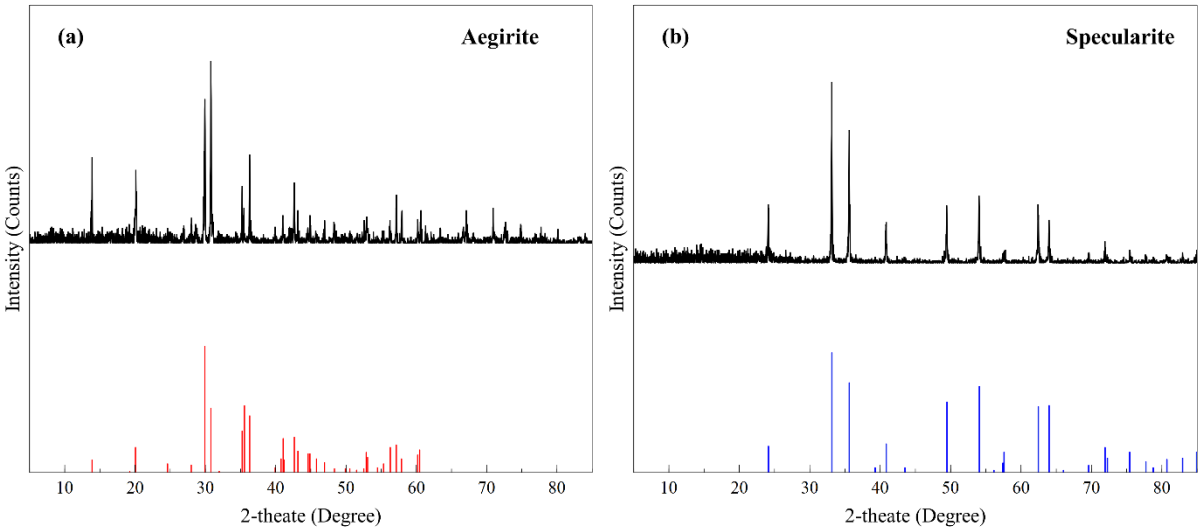

Fig. 2. XRD patterns of (a) aegirite and (b) specularite single mineral

2.2.2. Microflotation

For a typical flotation test, 2 g sample was added to the flotation cell containing 40 mL deionized water. After 3 min pH adjustment, a certain amount of depressant and collector was added successively with the time interval of 3 min for regent fully adsorption to mineral surface and the mechanical impeller speed, airflow rate, and flotation time was controlled at 1460 r/min, 180 mL/min, 5 min, respectively. The concentrate and tailings were then recovered, dried, and weighed for the subsequent analysis. For single mineral flotation tests, the recoveries were calculated according the weight of products as Eq (1). For the artificial mixed mineral (aegirite: specularite is 1:1 with a total mass weight of 2 g), the separation efficiency was adopted as Eq. (2):

$$R = \frac{m}{m_c + m_t} \tag{1}$$

$$S_E = R_m - R_t \tag{2}$$

where R and m represents recovery and the weight of concentrate or tailings, respectively; m_c and m_t donates the weight of concentrate and tailings, respectively; S_E, R_m and R_t donates separation efficiency, recovery of specularite, and recovery of tailings in concentrate, respectively.

2.2.3. Zeta potential measurements

Zeta potential measurements were carried out in a ZetaPALS potential analyzer (Brookhaven Instruments Ltd. US.). 5 mg of mineral sample (less than 2 μm) was added into 50 mL 1×10^{-3} mol/L KCl under stirring, then the depressant TGA or MPA was introduced and the concentration was adjusted to 40 mg/L. The pH of the slurry is regulated to the desired value and held for 2 min to a homogeneous phase before measurement. Each experiment was measured 3 times independently, and the average value was taken as the final result.

2.2.4. Adsorption experiment

The adsorption capacity of the depressants to the two minerals was determined by measuring the total carbon content (TOC) in the solution using a TOC-L analyzer (Shimadzu Japan). The residual concentration approach was used to detect the amount of depressant adsorbed on the mineral surface. Firstly, 2 g of specularite or aegirite was distributed equally in the depressant solution at pH 9 under stirring for 1h. Then the slurry was centrifuged, and the supernatant was utilized to determine the TOC content. The equation for the adsorption of the depressant to the two minerals is as Eq. (3):

$$Q = \frac{(C_0 - C_1) \times V}{W} \tag{3}$$

where Q (mg/g) is the adsorption amount of the depressant to mineral, C_0 (mg/L) and C_1 (mg/L) were the depressant concentrations before and after adsorption, correspondingly, W (g) represented the weight of mineral.

2.2.5. Contact angle measurement

The contact angle was determined using a JC2000A contact angle analyzer (Powereach Instruments, Shanghai, China). The lump of high-purity minerals were to a proper size, and then cut surface was polished via polishing paper before washing three times with deionized water. The prepared samples were immersed into the collector NaOl (60 mg/L) or depressant (40 mg/L of TGA or MPA) solution for 30 min, then were dried in vacuum at 40°C. A deionized water droplet of 3.0 μL was dropped on the mineral surface by using an automatic sample injection syringe and then the contact angle was measured by capturing images of the water droplet profile using Young-Laplace equation in a computer. The statistics obtained were the averages of five distinct measurements.

2.2.6. XPS analysis

Measurements of X-ray photoelectron spectroscopy (XPS) were performed by a Thermo ESCALAB 250XI X-ray photoelectron spectrometer (Thermo Fisher Scientific, USA). During the measurements, the monochromatic Al K radiation was used as the excitation source for the observations, with a pass energy of 100 eV and a 1 eV energy step size. Measurements and high-resolution spectra were recorded for O1s, C1s, Si 2p, and Fe 2p. The binding energy of C1s was calibrated to 284.6 eV during XPS analysis. The sample preparation for XPS measurements was carried out as follows: under stirring for 1 h, 1 g of specularite or aegirite with a size fraction of less than 2 μm was stirred in a 200 mL beaker, which contained 100 mL of 40 mg/L depressant solution at pH 9. The slurry was centrifuged, then dried in a vacuum oven at 25°C for 24 hours. The produced samples were pressed onto double-sided conductive adhesive carbon tapes for XPS measurements.

3. Results and discussion

3.1. Flotation results

Firstly, the specularite and aegirite were separated using collector NaOl. According to the results in Fig. 3 (a), with the 40 mg/L initial concentration of NaOl, the floatability of specularite increases with increasing slurry pH values from 3 to 6. In the pH range of 6-9, the floatability of specularite enters a plateau zone, and it starts to decrease when the pH is greater than 9. For aegirite, the recovery of aegirite is in the form of inverted V, and its floatability reached the optimum at pH 6. Because of the low ionization of NaOl in acidic conditions and metal species on mineral surfaces are highly hydroxylated under alkaline conditions, resulting in surface hydrophilicity variations and poor chemical adsorption, which leads to low floatability of the two minerals either under high acid or high alkali conditions. As a consequence, pH 9 produces the optimum separation findings for two minerals (recovery of specularite 65.83% and aegirite 26.87%).

As can be seen in Figure 3b, the desirable NaOl concentration for aegirite/specularite separation was determined at NaOl concentration ranging from 20 to 100 mg/L and a pH of 9. The recoveries of both minerals grew as the concentration of NaOl increased, as predicted. Their floatability remained stable when the NaOl concentration was above 60 mg/L, with 88.71% and 86.53% recoveries for specularite

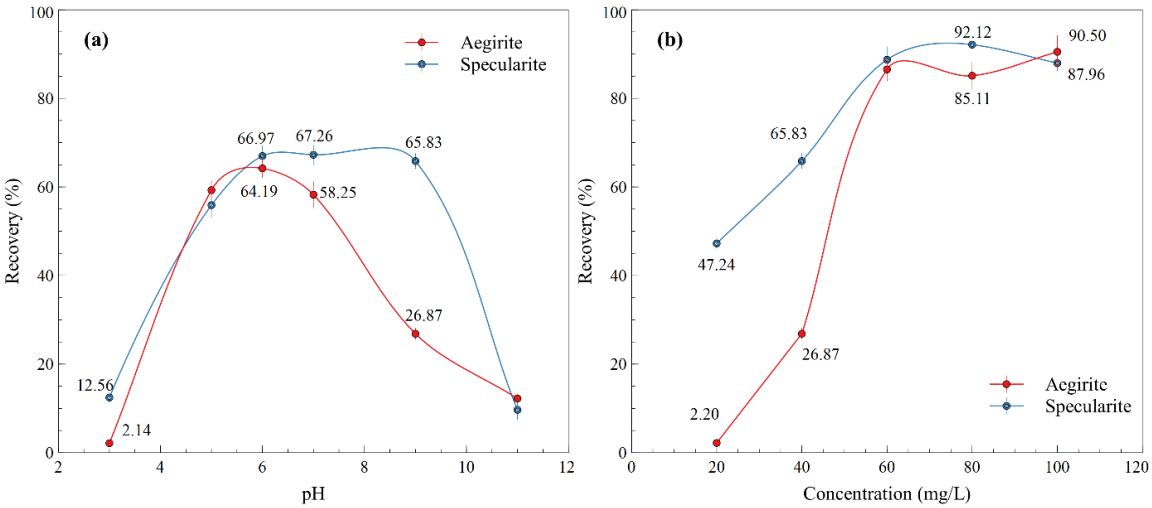

Fig. 3. The floatability of aegirite and specularite with (a) different pH values at 40 mg/L NaOl and (b) different NaOl concentration at pH 9

and aegirite, respectively. Thus, the optimal concentration of NaOl was picked to be 60 mg/L.

The separation performance of aegirite and specularite with collector but without depressant is unsatisfactory. Therefore, TGA and MPA were chosen as the depressants for aegirite/specularite separation with 60 mg/L NaOl at pH 9. The Fig. 4(a) suggests that the recovery of aegirite declined significantly as the TGA concentration was raised from 10 to 40 mg/L, while the floatability of specularite was not affected obviously. For example, the aegirite was absolutely depressed by 40 mg/L of TGA while the recovery of specularite was still as high as 76.30%. In addition, compared to the floatability of specularite without depressant, the recovery of specularite decreased around 10 percentage point when TGA was added. This demonstrates that, except aegirite, TGA exhibits a diminishing impact on specularite floating to a certain extent.

The two minerals' floatability with varied MPA concentrations is depicted in Fig. 4(b). It is similar to TGA that the recovery of aegirite declined as the concentration of MPA increased, whereas the recovery of specularite was virtually unaffected by MPA. The recovery of aegirite barely decreased from 59.36% to 47.70% as the MPA concentration increased from 0 to 40 mg/L, and the maximum separation gap was only 47.21 percentage point. Compared to TGA, the depression performance of MPA to aegirite and specularite was much weaker. Therefore, although TGA exhibits stronger depression performance to specularite than MPA, the total inhibitory selectivity and separation efficiency of TGA is much better than MPA.

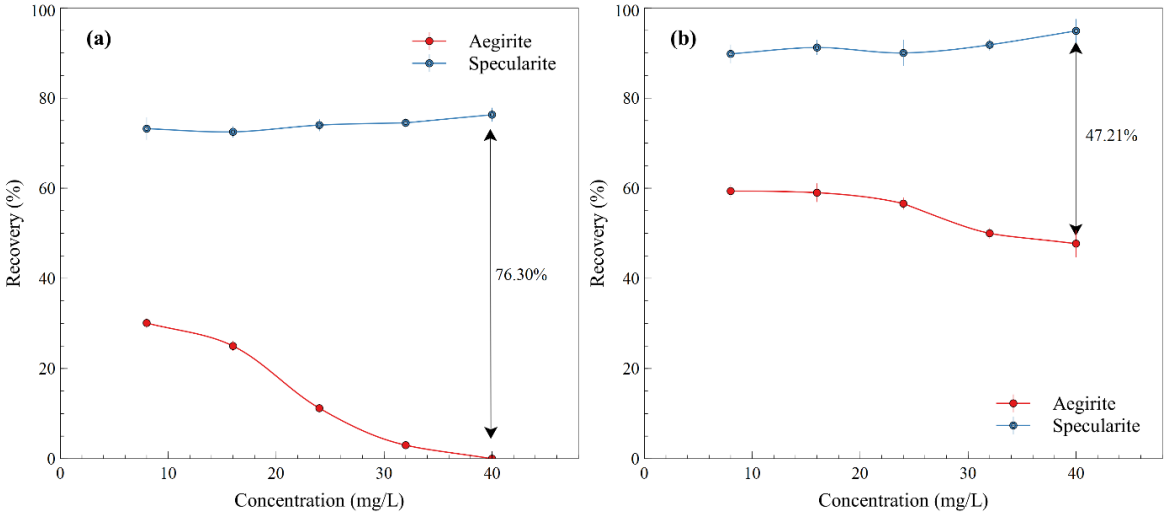

Fig. 4. The floatability of aegirite and specularite at 40 mg/L NaOl with (a) different TGA concentration and (b) different MPA concentration at pH 9

Because the single mineral flotation results prove that the two thiol depressants show good selectivity for the flotation separation of aegirite and specularite, further artificial mixed mineral flotation trials were undertaken to confirm the performance of the depressants at pH 9. The results in Table 2 show that as the dosage of two depressants was elevated, the yield and Fe recovery of rough concentrate dropped, while the Fe grade exhibited the opposite trend. This indicates that these two depressants have inhibited the flotation of aegirite in mixed minerals. In contrast, the Fe grade of rough concentrate increased by around 4 percentage point while Fe recovery dropped by about 7 percentage point with TGA as the depressant. For example, when the TGA and MPA dosage was 400 g/t, the separation efficiency of the mixed mineral was 69.57% and 64.02%, respectively. This indicated that TGA shows a higher selectivity than MPA, which is consistent with the single mineral flotation results.

Table 2. Flotation separation of mixed minerals with various TGA and MPA concentrations. (%)

Dosage (g/t)	Product	TGA			MPA		
		Yield	Fe Grade	Fe Recovery	Yield	Fe Grade	Fe Recovery
240	Rough Concentrates	75.33	50.13	84.32	86.76	47.06	91.75
	Tailings	24.67	28.47	15.68	13.24	27.72	8.25
	Feed	100	44.79	100.00	100	44.50	100.00
320	Rough Concentrates	70.25	52.43	82.04	83.83	48.11	89.76
	Tailings	29.75	27.11	17.96	16.17	28.44	10.24
	Feed	100	44.90	100.00	100	44.93	100.00
400	Rough Concentrates	65.29	53.95	78.33	80.32	49.27	87.54
	Tailings	34.71	28.08	21.67	19.68	28.62	12.46
	Feed	100	44.97	100.00	100	45.21	100.00
480	Rough Concentrates	61.82	55.14	75.63	76.24	49.65	84.43
	Tailings	38.18	28.77	24.37	23.76	29.39	15.57
	Feed	100	45.07	100.00	100	44.84	100.00
560	Rough Concentrates	59.46	55.81	73.69	71.48	51.16	81.22
	Tailings	40.54	29.22	26.31	28.52	29.64	18.78
	Feed	100	45.03	100.00	100	45.02	100.00

3.2. Zeta potential measurements

Fig. 5(a) describes the zeta potential of aegirite in the presence and absence of collectors and depressants as a function of pH. The zeta potential of aegirite declined with rising pH in the pH range investigated, which is in excellent agreement with previous research (Li, 2019). The addition of NaOl alone produced a more negative zeta potential, reflecting that adsorption of NaOl on the aegirite occurred. With the inclusion of TGA or MPA, the zeta potential values were converged to the one with NaOl only, illustrating that these two depressants could adsorb on aegirite effectively, thereby the floatability of aegirite declined sharply.

The Fig. 5(b) displayed the Zeta potential of specularite treated under varying reagent conditions. The Zeta potential of specularite without reagent showed a decreasing trend with increasing pH and the isoelectric point appeared at around 4.5, which was consistent with previous literatures (Li, 2020). The zeta potential of specularite is substantially decreased by introducing NaOl, indicating the adsorption of NaOl. Notably, when TGA or MPA was added, the Zeta potential value was comparable to pure specularite, which demonstrated the adsorption of TGA and MPA on the surface of the

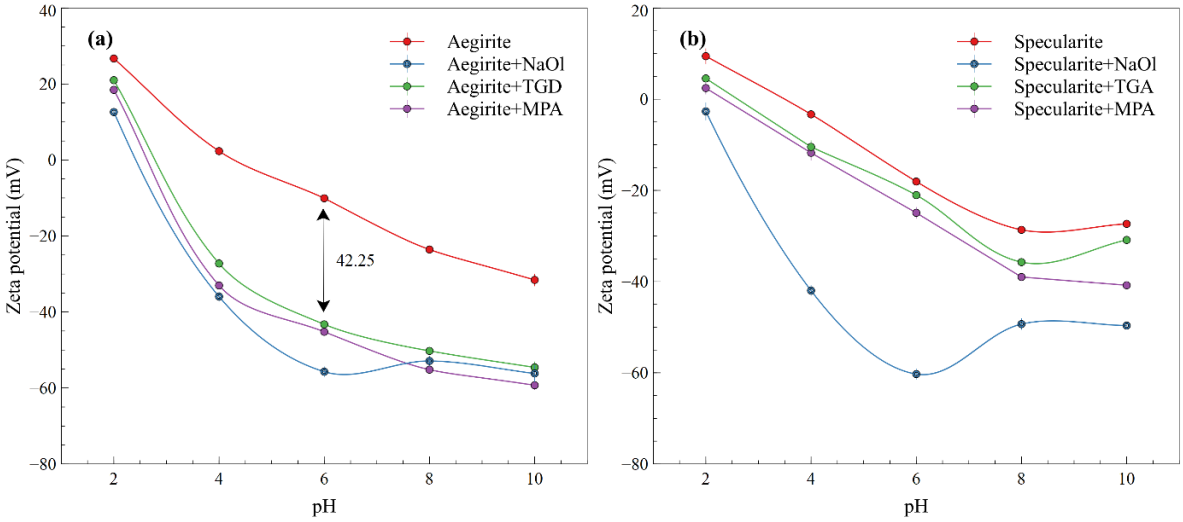

Fig. 5. The Zeta potential of (a) aegirite and (b) specularite with addition of TGA and MPA

specularite is weak. In other words, TGA and MPA would adsorb selectively on aegirite's surface, resulting in strong depression on aegirite.

3.3. Adsorption measurements

Fig 6 presents the adsorption amount of TGA and MPA on the two mineral surface at different concentration. Distinctly, the adsorption amount of TGA or MPA on aegirite surface was about two times higher than that on specularite in the concentration range of 30-40 mg/L. This phenomenon explained effectively the separation performance and Zeta potential measurements, and demonstrated that the adsorption of TGA or MPA on aegirite leaded to the selective depression effect. By comparing TGA and MPA, the adsorption mass of MPA to the two minerals was higher than that of TGA, especially to aegirite. This may be due to the fact that the MPA molecule has one more carbon atom than the TGA molecule.

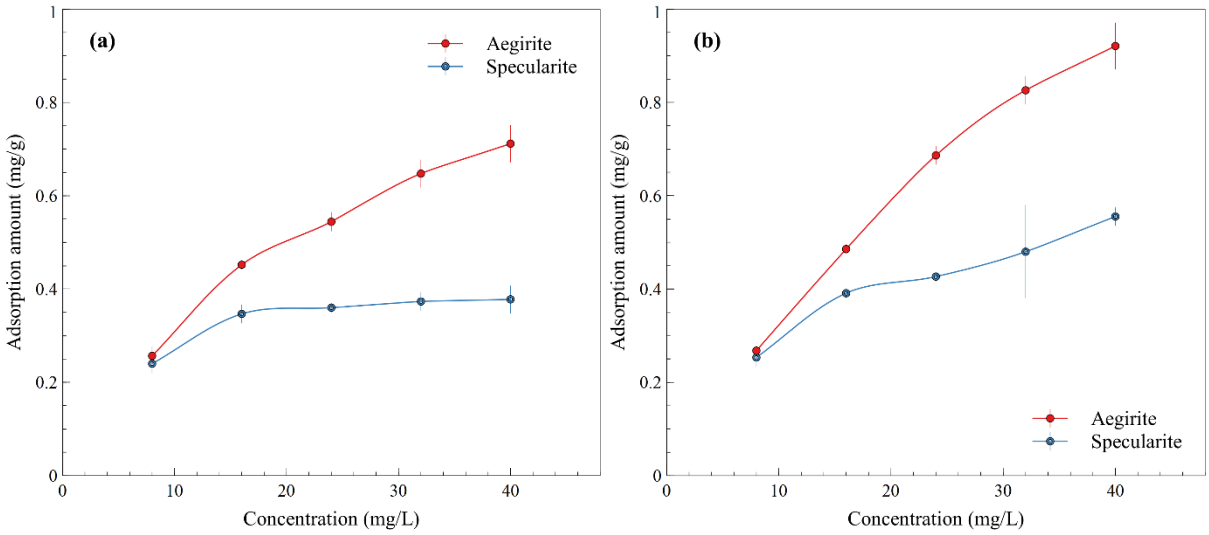

Fig. 6. The adsorption amount of (a) TGA and (b) MPA on aegirite and specularite as a function of concentration

3.4. Contact angle measurements

The difference in minerals' floatability is directly related to the surface wettability after modification by flotation reagent, and the contact angle can quantitatively describe the difference in wettability (Yang, 2020). It has been accepted that a mineral surface with higher water contact angle exhibits better hydrophobicity and floatability (Wang, 2021). The contact angle of aegirite and specularite before and

after treatment with NaOl, TGA, MPA and the combination of NaOl and depressant was measured to analyze their different flotation behaviors, as shown in Table 3. Results of contact angle measurement indicated that the contact angle of specularite and aegirite was observed to be 50.4° and 43.3°, respectively, suggesting lower natural hydrophilicity of specularite than aegirite. The contact angle of specularite and aegirite raised to 67.3° and 64.8°, respectively, after modified with NaOl, implied that the adsorption of NaOl improved hydrophobicity of these two minerals, which was in agreement with the high recovery of flotation. The addition of TGA or MPA remarkably decreased the contact angle of aegirite, which depicted that these two depressants was intensely able to cover the aegirite surface. Although the contact angle of specularite decreased likewise, the descent range was much smaller than that of aegirite. Furthermore, the addition of NaOl after depressant largely restored the contact angle of specularite, but the contact angle of aegirite slightly hardly changed. These results demonstrated that the TGA or MPA could adsorb on aegirite surface, interfering with the following adsorption of NaOl, thereby rendering the aegirite surface hydrophobic.

Table 3 Contact angle measurement results (pH=9; NaOl concentration: 60 mg/L; TGA or MPA concentration: 40 mg/L).

Test system	Specularite (°)	Aegirite (°)
Without reagent	50.4	43.3
With NaOl	67.3	64.8
With TGA	41.7	18.6
With MPA	44.3	22.4
With TGA+NaOl	56.1	23.5
With MPA+NaOl	61.4	32.3

3.5. XPS analyses

As a sensitive quantitative spectroscopic technique for the adsorption mechanism analysis of reagent on the surface of the mineral before and after reaction, XPS tests were performed to further illustrate the mechanism of interaction between the two depressants and aegirite. Fig. 7 displayed the survey scan XPS spectra of aegirite before and after TGA and MPA treatment. On the aegirite surface, metal atom peaks including Na 1s, Fe 2p, and Si 2p can be observed. Atomic concentrations of S increased from 0.21% to 0.83% and 0.88%, respectively, after addition of TGA and MPA, which was originated from the thiol group in TGA and MPA molecules, verifying the adsorption of the depressants.

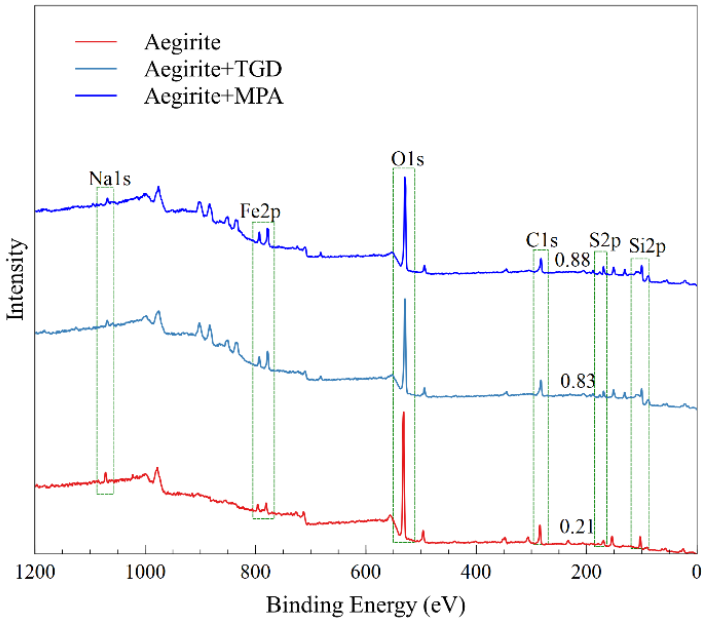

Fig. 7. XPS spectra of aegirite with and without being treated by TGD or MPA

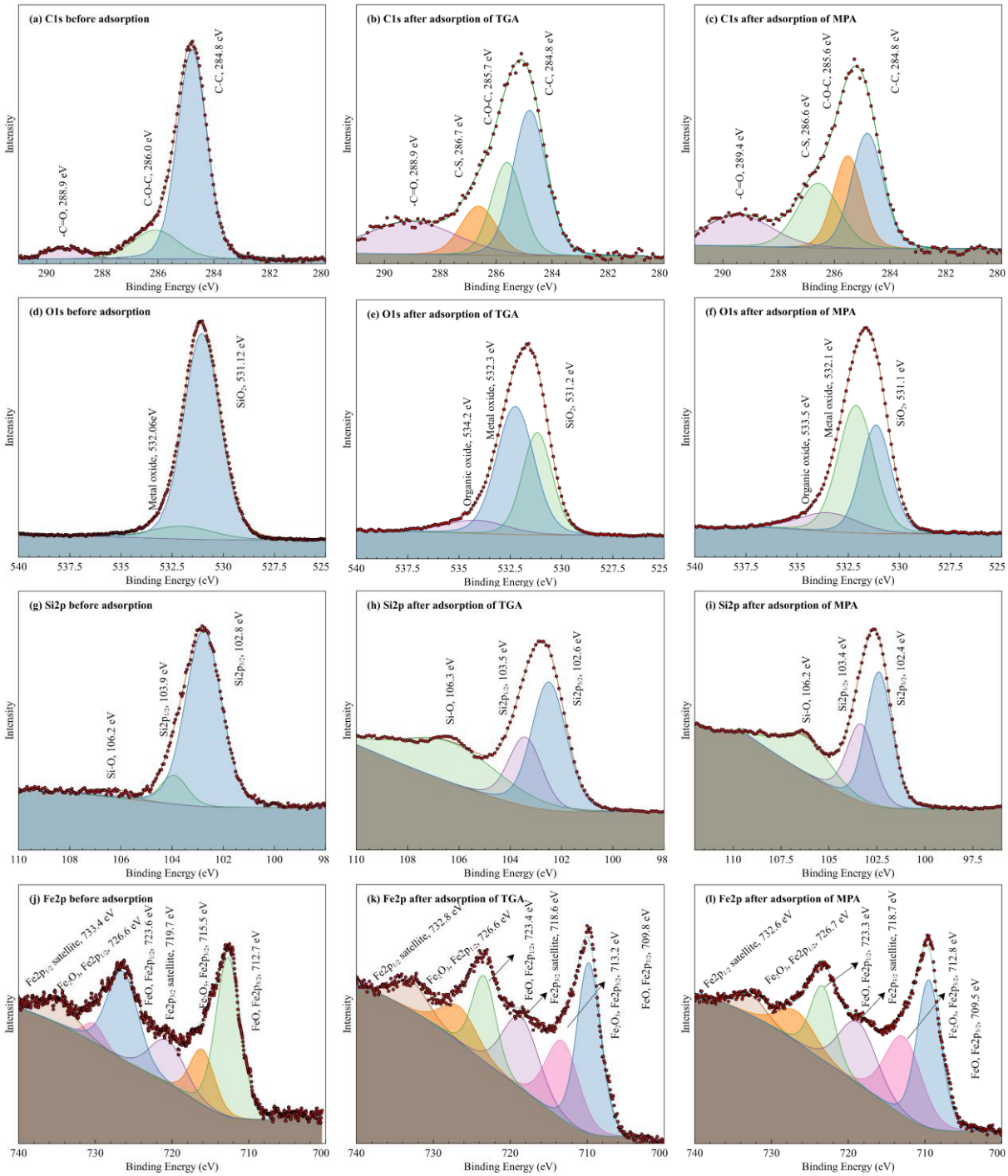

Fig. 8. High-resolution spectra of XPS on C 1s, O 1s, Si 2p, and Fe 2p before and after TGA or MPA adsorption

Fig. 8 reflects the absolute resolution XPS spectra of C 1s, O 1s, Si 2p, and Fe 2p for aegirite before and after TGA and MPA treatment, as well as their deconvoluted fitting curves. The binding energy (BE) peaks in Fig. 8(a) at 284.8, 286.0, and 288.9 eV are assigned to C-C, C-O-C, and C=O, separately, in the C 1s spectrum (Gao, 2020). The new peak at 286.7 eV in Fig. 8(b) and 8(c) corresponds to the thiol groups from TGA and MPA. Moreover, the intensity of C=O increased distinctly due to the carboxyl groups in the depressant molecule. After adsorbing MPA, the C=O peaks migrated to a higher location, indicating that carboxyl groups and metals on the aegirite surface interacted and served as electron donors throughout the adsorption process.. For O 1s spectrum, the new peaks at 534.2 and 533.5 eV are allocated to carboxyl groups from TGA and MPA. The intensity increase of Si-O at 106.2 eV significantly, which was due to the reaction between carboxyl groups in the depressant molecule and Si in aegirite

surface. The corresponding BE peaks at 726.6 and 715.5 eV are for Fe (III) $2p_{1/2}$, and Fe (III) $2p_{3/2}$, respectively; 733.4 and 719.7 V are for Fe (III) $2p_{1/2}$ satellite, and Fe (III) $2p_{3/2}$ satellite, respectively (Biesinger, 2011; Uhlig, 2001). There four deconvoluted peaks migrated to lower binding energies to a certain extent, indicating that iron absorbed electrons during TGA or MPA adsorption process. XPS results confirmed that TGA or MPA donated electrons to Fe and Si in aegirite surface in the adsorption process and alters aegirite's surface properties and depresses it during flotation processes.

3.6. HLB calculation

The hydrophilic-lipophilic balance (HLB) (Davies, 2012) number is defined in terms of the number assigned to the chemical groups in a surfactant, as follows:

$$\mathrm{HLB}=7+\sum(\text{hydrophilic group numbers})-\sum(\text{hydrophobic group numbers}) \quad (4)$$

According to the reported group numbers by Goodwin (Goodwin, 2009), the HLB of NaOl, TGA, and MPA is 1.03, 10.13, and 9.65, respectively. This suggests that the hydrophilicity of TGA and MPA is much higher than NaOl, thus the adsorption of TGA and MPA would increase the hydrophilicity of mineral and depress its attachment to air bubbles. Additionally, the HBL of TGA is higher than MPA, which leads TGA stronger depression performance to specularite/aegirite than MPA.

4. Conclusions

This research involves comparison investigation of two thiol-type reagents TGA and MPA as depressants to improve the separation of specularite/aegirite via direct flotation. TGA and MPA exhibited satisfactory selective depression for aegirite with recovery of 0% and 47.21%, respectively, with 60 mg/L NaOl at pH 9. However, the floatability of specularite still stay high with recovery of 76.30% and 94.91%, respectively, at the same condition. The higher HLB of TGA contributed to the more excellent depression performance for specularite/aegirite separation than MPA. Mechanism investigation have manifested that TGA and MPA can be selectively adsorb on aegirite surface through interaction between depressant and Si and Fe atoms, which blocked the NaOl's subsequent adsorption and lead to the floatability difference between specularite and aegirite.

Acknowledgements

This work was supported by the financial support from the National Natural Science Foundation of China (51904001), China Postdoctoral Science Foundation funded project (2020M673590XB) and the Open Project Program of State Key Laboratory of Complex Nonferrous Metal Resources Clean Utilization (CNMRCUKF2202).

References

FILIPPOV, L. O., SEVEROV, V. V., FILIPPOVA, I. V., 2013. *Mechanism of starch adsorption on Fe–Mg–Al-bearing amphiboles*. International Journal of Mineral Processing, 123, 120–128.

FU, Y., YIN, W., YANG, B., LI, C., ZHU, Z., LI, D., 2018. *Effect of sodium alginate on reverse flotation of hematite and its mechanism*. International Journal of Minerals Metallurgy and Materials, 25(10), 1113–1122.

LI, M., LIU, J., HU, Y., GAO, X., YUAN, Q., ZHAO, F., 2020. *Investigation of the specularite/chlorite separation using chitosan as a novel depressant by direct flotation*. Carbohydrate Polymers, 240, 116334.

WENG, X., MEI, G., ZHAO, T., & ZHU, Y., 2013. *Utilization of novel ester-containing quaternary ammonium surfactant as cationic collector for iron ore flotation*. Separation and Purification Technology, 103, 187-194.

PEREIRA, A. R. M., HACHA, R. R., TOREM, M. L., MERMA, A. G., SILVAS, F. P., 2021. *Direct hematite flotation from an iron ore tailing using an innovative biosurfactant*. Separation Science and Technology, 56(17), 2978-2988.

LI, M., LIU, J., GAO, X., HU, Y., TONG, X., ZHAO, F., YUAN, Q., 2019. *Surface properties and floatability comparison of aegirite and specularite by density functional theory study and experiment*. Minerals, 9(12), 782.

LI, M., YANG, R., GAO, X., & HU, Y., 2020. *The effect of selective adsorption of dissolved aegirite species on the separation of specularite and aegirite*. Advanced Powder Technology, 31(10), 4197-4206.

ZHANG, C., XU, Z., HU, Y., HE, J., TIAN, M., ZHOU, J., ZHOU, Q., CHEN, S., CHEN, D., CHEN P., W., 2019. *Novel insights into the hydroxylation behaviors of a-quartz (101) surface and its effects on the adsorption of sodium oleate*. Minerals, 9(7), 450.

YANG, B., YIN, W., YAO, J., SHENG, Q., ZHU, Z., 2022. *Role of decaethoxylated stearylamine in the selective flotation of hornblende and siderite: An experimental and molecular dynamics simulation study*. Applied Surface Science, 571, 151177.

ROCHA, G. M., de Souza MACHADO, N. R., PEREIRA, C. A., 2019. *Effect of ground corn and cassava flour on the flotation of iron ore tailings.* Journal of Materials Research and Technology, 8(1), 1510-1514.

YAO, J., YIN, W., & GONG, E., 2016. *Depressing effect of fine hydrophilic particles on magnesite reverse flotation*. International Journal of Mineral Processing, 149, 84-93.

SHRIMALI, K., & MILLER, J. D., 2016. *Polysaccharide depressants for the reverse flotation of iron ore*. Transactions of the Indian Institute of Metals, 69(1), 83-95.

POPERECHNIKOVA, O. Y., FILIPPOV, L. O., SHUMSKAYA, E. N., & FILIPPOVA, I. V., 2017. *Intensification of the reverse cationic flotation of hematite ores with optimization of process and hydrodynamic parameters of flotation cell.* In Journal of Physics: Conference Series, 879(1), 012016.

LUO, X. M., YIN, W. Z., WANG, Y. F., SUN, C. Y., MA, Y. Q., LIU, J., 2016. *Effect and mechanism of siderite on reverse anionic flotation of quartz from hematite*. Journal of Central South University, 23(1), 52-58.

VELOSO, C. H., FILIPPOV, L. O., FILIPPOVA, I. V., OUVRARD, S., ARAUJO, A. C., 2018. *Investigation of the interaction mechanism of depressants in the reverse cationic flotation of complex iron ores*. Minerals Engineering, 125, 133-139.

LI, M., LIU, J., HU, Y., GAO, X., YUAN, Q., ZHAO, F., 2020. *Investigation of the specularite/chlorite separation using chitosan as a novel depressant by direct flotation*. Carbohydrate polymers, 240, 116334.

HUANG, G., ZHOU, C., LIU, J., 2012. *Effects of different factors during the de-silication of diaspore by direct flotation.* International Journal of Mining Science and Technology, 22(3), 341-344.

MONTES-SOTOMAYOR, S., HOUOT, R., KONGOLO, M., 1998. *Flotation of silicated gangue iron ores: Mechanism and effect of starch*. Minerals Engineering, 11(1), 71–76.

MOREIRA, G. F., PEÇANHA, E. R., MONTE, M. B. M., LEAL FILHO, L. S., STAVALE, F., 2017. *XPS study on the mechanism of starch-hematite surface chemical complexation*. Minerals Engineering, 110, 96–103.

LI, L., ZHANG, C., YUAN, Z., XU, X., SONG, Z., 2019. *AFM and DFT study of depression of hematite in oleate-starch-hematite flotation system.* Applied Surface Science, 480, 749–758.

GIBBS, H. L., 1948. U.S. Patent No. 2,449,984. Washington, DC: U.S. Patent and Trademark Office.

LIU, Q., 1985. *Studies on the flotation depression of chalcopyrite, galena and sphalerite by thioglycollic acid* (Doctoral dissertation, University of British Columbia).

LI, M. Y., WEI, D. Z., SHEN, Y. B., LIU, W. G., GAO, S. L., Liang, G. Q., 2015. *Selective depression effect in flotation separation of copper–molybdenum sulfides using 2, 3-disulfanylbutanedioic acid.* Transactions of Nonferrous Metals Society of China, 25(9), 3126-3132.

YIN, Z., SUN, W., HU, Y., ZHAI, J., GUAN, Q., 2017a. *Evaluation of the replacement of NaCN with depressant mixtures in the separation of copper-molybdenum sulphide ore by flotation*. Separation and Purification Technology, 173, 9–16.

YIN, Z., XU, L., HE, J., WU, H., FANG, S., KHOSO, S. A., HU, Y. H., SUN, W., 2019b. *Evaluation of l-cysteine as an eco-friendly depressant for the selective separation of MoS_2 from PbS by flotation*. Journal of Molecular Liquids, 282, 177-186.

YAN, H., YANG, B., ZHU, H., HUANG, P., HU, Y., 2021. *Selective flotation of Cu-Mo sulfides using dithiothreitol as an environmental-friendly depressant*. Minerals Engineering, 168, 106929.

LI, M., YUAN, Q., GAO, X., HU, Y. (2020). *Understanding the differential depression of tetrasodium glutamate diacetate on the separation of specularite and chlorite: Experimental and DFT study*. Minerals Engineering, 159, 106629.

YANG, B., WANG, D., CAO, S., YIN, W., XUE, J., ZHU, Z., FU, Y. YAO, J., 2020. *Selective adsorption of a high-performance depressant onto dolomite causing effective flotation separation of magnesite from dolomite.* Journal of Colloid and Interface Science, 578, 290-303.

WANG, X., LIU, J., ZHU, Y., HAN, Y. (2021). *Adsorption and depression mechanism of an eco-friendly depressant PCA onto chalcopyrite and pyrite for the efficiency flotation separation.* Colloids and Surfaces A: Physicochemical and Engineering Aspects, 620, 126574.

GAO, X., LIU, J., LI, M., GUO, C., LONG, H., ZHANG, Y., XIN, L. (2020). *Mechanistic study of selective adsorption and reduction of Au (III) to gold nanoparticles by ion-imprinted porous alginate microspheres.* Chemical Engineering Journal, 385, 123897.

BIESINGER, M. C., PAYNE, B. P., GROSVENOR, A. P., LAU, L. W., GERSON, A. R., SMART, R. S. C., 2011. *Resolving surface chemical states in XPS analysis of first row transition metals, oxides and hydroxides: Cr, Mn, Fe, Co and Ni.* Applied Surface Science, 257(7), 2717-2730.

UHLIG, I., SZARGAN, R., NESBITT, H. W., & LAAJALEHTO, K., 2001. *Surface states and reactivity of pyrite and marcasite.* Applied Surface Science, 179(1-4), 222-229.

GOODWIN, J., 2009. Colloids and interfaces with surfactants and polymers. John Wiley & Sons.

DAVIES, J. T., 2012. Interfacial phenomena. Elsevier.